Measurement of the total cross section and ρ-parameter from elastic scattering at $\sqrt{s} = 13$ TeV in ATLAS

D. Caforio

II. Physikalisches Institut
Justus-Liebig-Universität, Giessen

LHC Forward Physics meeting - 25.10.2022

Elastic scattering with the ALFA detector

Measuring the total cross section and the ρ-parameter in the nuclear region

σ_{tot} non computable in perturbative QCD, but can be measured using the Optical Theorem:

$$\sigma^2_{tot} = \frac{16\ \pi}{1+\rho^2} \frac{d\sigma_{el}}{dt}\bigg|_{t\to 0}$$

related through dispersion relations to the nuclear slope ρ-parameter, derived from unitarity and analycity of scattering amplitudes:

$$\rho = \frac{Re\ f_N(0)}{Im\ f_N(0)}$$

Theoretical predictions

$$\frac{d\sigma}{dt} = \frac{1}{16\pi}\left|f_N(t) + f_C(t)e^{i\alpha\phi(t)}\right|^2$$

$$f_C(t) = -8\pi\alpha\hbar c \frac{G^2(t)}{|t|}$$

$$f_N(t) = (\rho + i)\frac{\sigma_{tot}}{\hbar c} e^{(-B|t| - C|t|^2 - D|t|^3)/2}$$

$$\rho = \frac{Re\ f_N(0)}{Im\ f_N(0)}$$

The ALFA detector

The ALFA detector to measure elastic scattering in *pp* collisions:

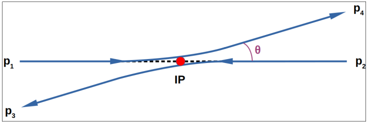

$$t = (p_1 - p_3)^2 = (p_2 - p_4)^2$$
$$\approx -(p\theta)^2$$

θ very small, order of microrad

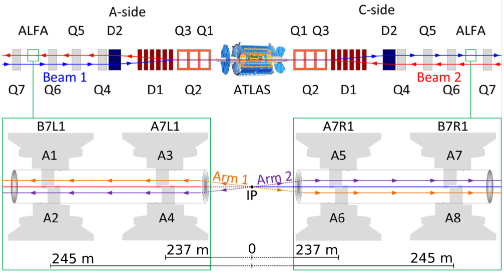

- 2 Roman Pot stations on each side of IP, 2 tracking detectors (scintillating fibers) in each station
- Main Detectors (MDs) to measure scattered protons, Overlap Detectors (ODs) for alignment
- the detectors are moved very close to the beam, down to 3.5 σ

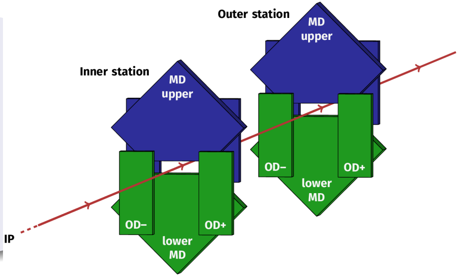

Measurement principle

- 4 dedicated fills at $\beta^\star = 2500$ m to access the CNI region
- $\sqrt{s} = 13$ TeV, int. luminosity 340 $\mu\mathrm{b}^{-1}$, 6.8 million elastic scattering candidates
- phase advance $\Psi = 90^\circ$ between the IP and the RPs $\Rightarrow$ "parallel-to-point focusing" (in the vertical plane only)

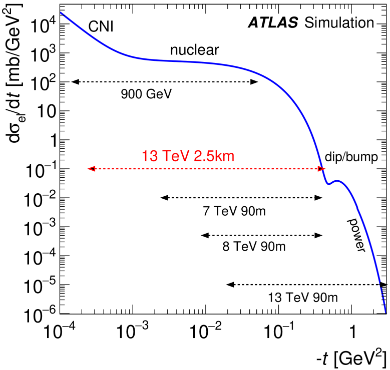

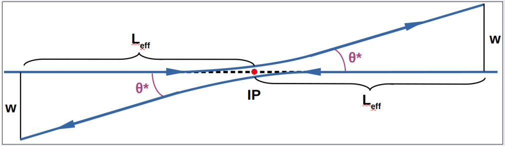

trajectory (w, θ_w) given by the transport matrix **M** and the coordinates at the IP $(w^\star, \theta^\star_w)$:

$$\begin{pmatrix} w \\ \theta_w \end{pmatrix} = \begin{pmatrix} M_{11} & M_{12} \\ M_{21} & M_{22} \end{pmatrix} \begin{pmatrix} w^\star \\ \theta^\star_w \end{pmatrix}$$

$$w = x,\ y$$

t-reconstruction

Four methods:

- subtraction: exploiting the back-to-back topology of elastic scattering
- local angle: local angle of the tracks measured between the inner and outer stations on the same side
- local subtraction method: using measurements at the inner and the outer stations, separately on the A-side and C-side, then combining the two sides
- lattice method: using both the measured positions and the local angle by inversion of the transport matrix

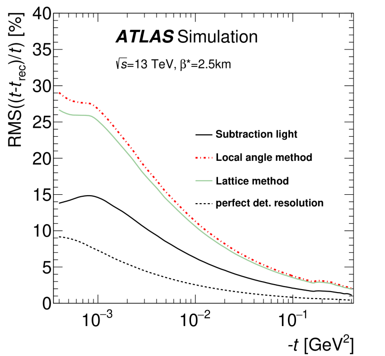

$$-t = \left[(\theta_x^\star)^2 + (\theta_y^\star)^2\right] p^2$$

$\theta_y^\star$ always reconstructed with the subtraction method (parallel-to-point focusing in the vertical plane), $\theta_x^\star$ reconstructed using all four methods

performance depends on the resolution: the subtraction method gets small contributions from the detector resolution (good for the space coordinates), all other methods suffer from local angle poorly measured (the 8 m distance between the two stations too small to obtain good precision)

Acceptance

- the distance to the beam determines the smallest accessible t, obtained at the detector edge
- acceptance is calculated from simulation, mainly determined by the geometry of the ALFA detector and the distance to the beam
- the t-spectrum is unfolded for detector resolution and beam divergence

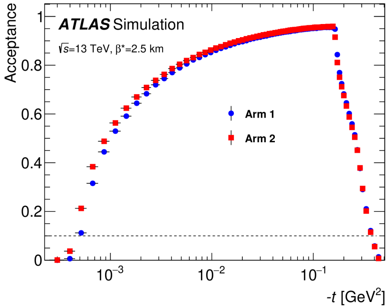

the shape of the acceptance curve determined by the contributions of the vertical and horizontal scattering angles to t:

small close to the edge: a fraction of the events are lost due to the beam divergence

maximum acceptance for events occurring at the largest possible values of $|y|$ within the beam-screen cut

beyond that point acceptance decreases steadily: the events are required to have larger values of $|x|$, these t-values dominated by the horizontal scattering angle component

difference between the two arms is mainly related to the vertical beam offset

Event selection and background estimation

- preselection: data quality, trigger and reconstruction requirements
- edge cut, beam screen shadow cut also applied
- the final selection exploits the back-to-back topology of elastic events

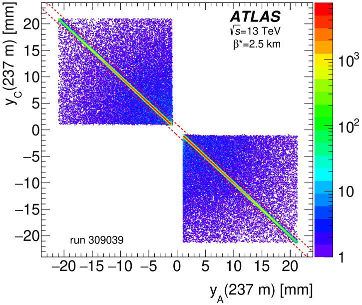

correlation of the y coordinate measured in the inner stations on the A-side and C-side (after preselection and fiducial cuts, before acceptance and background rejection)

elastic-scattering candidates observed in a narrow region along the diagonal, events are selected in a band of 2 mm width

Event selection and background estimation

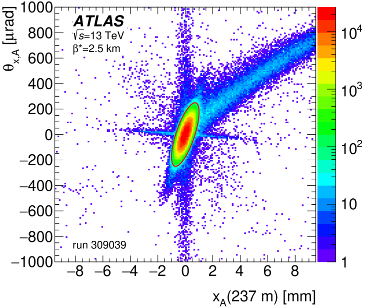

correlation between the coordinate and the local angle in the horizontal plane (after preselection and fiducial cuts, before acceptance and background rejection cuts)

identified elastic events are required to lie inside an ellipse corresponding to a 3.5σ selection

Background estimation

Event selection exploiting strong correlations present in elastic events

Sources of background considered:

- accidental halo+halo and halo+SD coincidences (data-driven, determined from single-side templates with an event-mixing method)
- central diffraction (DPE, MC simulation)

normalized in control regions in the data

systematics estimated by changing the normalization regions, the template composition, and the parameters of the DPE simulation

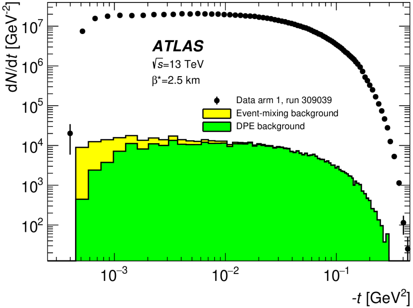

background level is 0.75‰ on average, relative uncertainty of 10 - 15%

Reconstruction efficiency

Reconstruction efficiency accounts for the elastic events which cannot be fully reconstructed and need to be excluded from the analysis

number of elastically scattered protons that are lost is estimated by a data-driven tag-and-probe method

this method exploits the back-to-back topology of elastic events, allowing a proton to be tagged on one side of the spectrometer and probe the reconstruction on the other side

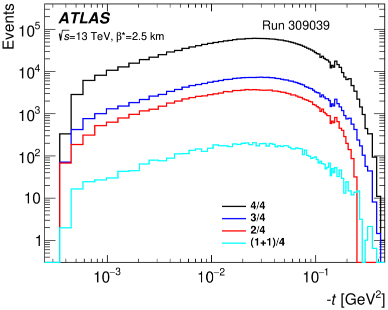

six reconstruction cases, or "topologies", named 4/4, 3/4, 2/4, (1+1)/4, 1/4 and 0/4

the numerator indicates the number of detectors with at least one reconstructed track

$$\epsilon_{rec} = \frac{N_{reco}}{N_{reco} + N_{fail}}$$

N_{reco} number of fully reconstructed elastic-scattering events

N_{fail} number of not fully reconstructed elastic-scattering events

Reconstruction efficiency

final reconstruction efficiency calculated per run and per arm

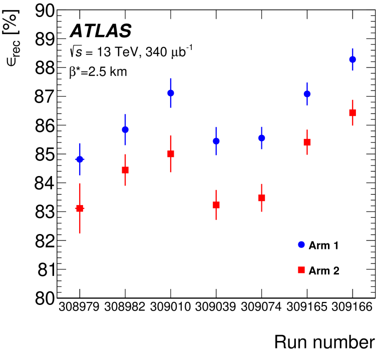

systematics range between 0.4% and 0.9% and are dominated by the composition of the templates for accidental coincidences and uncertainties in the background subtraction

the former are evaluated by applying different veto conditions and by increasing and decreasing the SD fraction in the template; the latter are calculated by varying the background normalization regions

Alignment

- rotation, horizontal and vertical offsets obtained from the left-right and up–down symmetry of the elastic pattern
- due to high sensitivity to distance uncertainties, a multi-step procedure for distance evaluation is performed: full analysis repeated assuming different values of the global vertical distance
- a fit to the differential elastic cross section is performed using only statistical uncertainties

- the χ^2 of the fit has a clear minimum whose position determines the final vertical distance used in the analysis
- the correction is found to be 86 μm, the uncertainty is evaluated to be 22 μm, the largest contribution originating from the variation of the luminosity within its uncertainty
- the vertical position of the beam between the elastic arms is fine-tuned by equalizing the t-spectra measured in the two arms
- the resulting uncertainty is improved to 4-15 μm, with corrections of the order of 12-27 μm

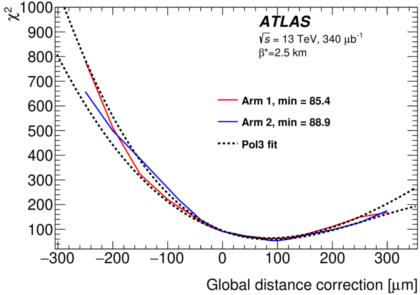

Beam optics

the reconstruction of the *t*-value requires knowledge of the elements of the transport matrix, that can be calculated from the design of the 2.5 km beam optics

the next step is to apply corrections to this "design" optics using constraints from the data: the reconstructed scattering angle must be the same for different reconstruction methods using different transport matrix elements

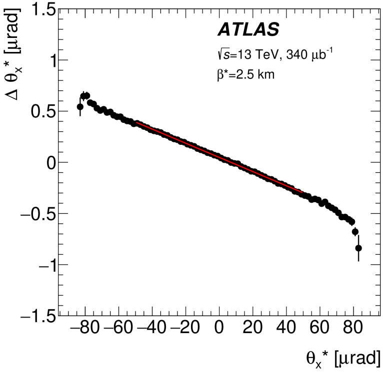

difference in reconstructed scattering angle $\Delta\theta_x^*$ between the subtraction and local angle methods as a function of the scattering angle using the subtraction method for the outer detectors

Beam optics

the “effective” beam optics parameters are determined from a global fit, using these constraints, with the design optics as starting value

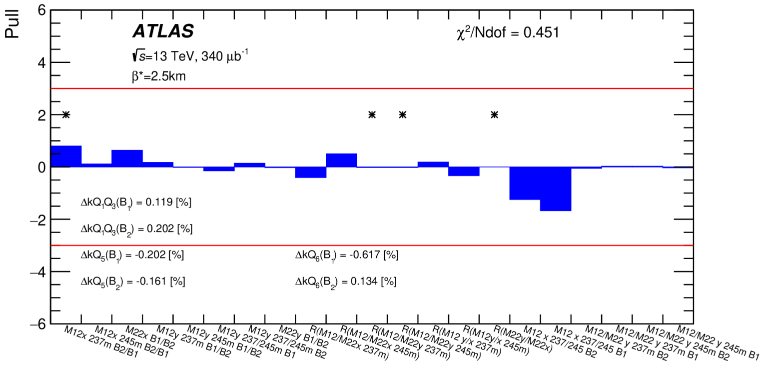

pulls from the effective beam optics fit of quadrupoles Q1, Q3, Q5 and Q6 to the ALFA constraints

Luminosity measurement

reliable luminosity determination by comparing the measurements of different detectors and algorithms

LUCID (*LUCID_EventORC_BI*) as the baseline; Beam Conditions Monitor and the Inner Detector to evaluate the systematic uncertainties

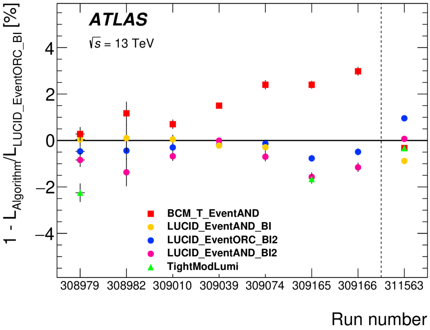

percentage deviation of the integrated luminosity with respect to the reference algorithm LUCID_EventORC_BI for all runs used in this analysis

main sources of systematic uncertainty: vdM calibration, calibration transfer, long-term stability and background; total systematic uncertainty: 2.15%

final value of the integrated luminosity: 339.9 $\pm$ 0.1 (stat.) $\pm$ 7.3 (syst.) $\mu\mathrm{b}^{-1}$

Differential elastic cross section

$$\frac{d\sigma}{dt_i} = \frac{1}{\Delta t_i} \times \frac{M^{-1}(N_1 - B_i)}{A_i \times \epsilon^{reco} \times \epsilon^{trig} \times \epsilon^{DAQ} \times L_{int}}$$

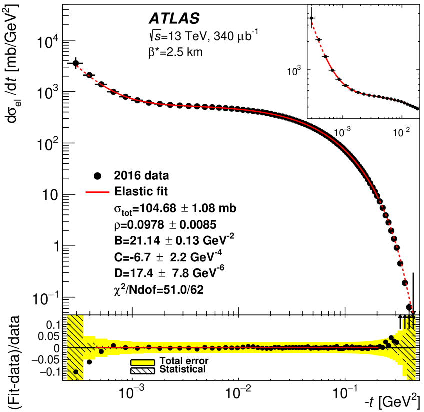

- reconstructed with the subtraction method
- fit of the BCD-model with σ_{tot}, ρ, B, C and D as free parameters
- experimental systematic uncertainties included in the profile fit $\Rightarrow$ included in the fit parameter errors
- dotted red line: extrapolation of the fit outside the fit range
- systematic uncertainties evaluated as function of t

Differential elastic cross section: systematics

main sources of systematic uncertainties: alignment, luminosity, reconstruction efficiency

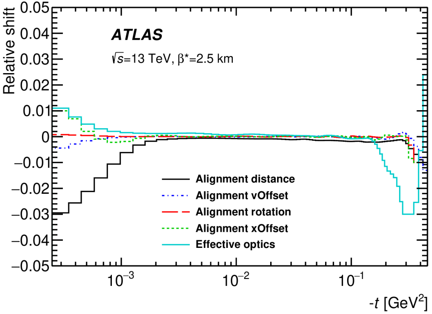

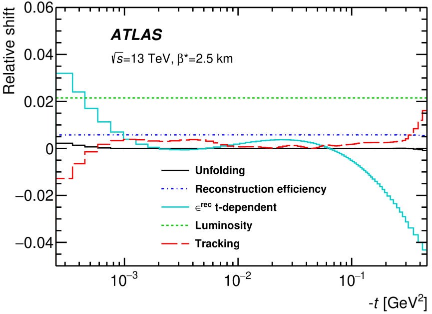

Differential elastic cross section: systematics

Checks on stability:

- time dependence
- fit range
- different t-reconstruction methods
- difference between arms

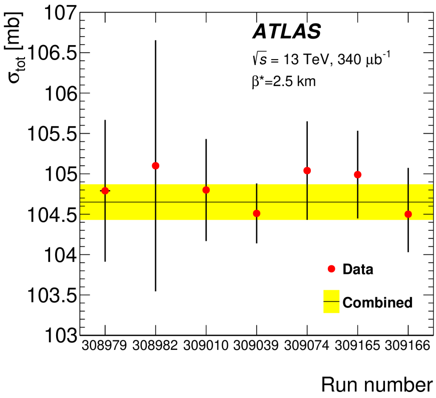

Differential elastic cross section: theory uncert.

	σ_{tot} [mb]	ρ	B [GeV^{-2}]	C [GeV^{-4}]	D [GeV^{-6}]
Central value	104.68	0.0978	21.14	−6.7	17.4
Statistical error	0.22	0.0043	0.07	1.1	3.8
Experimental error	1.06	0.0073	0.11	1.9	6.8
Theoretical error	0.12	0.0064	0.01	0.04	0.15
Total error	1.09	0.0106	0.13	2.3	7.8

Theoretical uncertainties

- parametrization of the strong amplitude
- Coulomb phase
- proton form factor
- nuclear phase

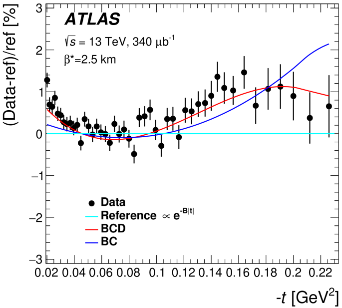

evidence for a t-dependent nuclear slope

Results: total elastic and inelastic cross section

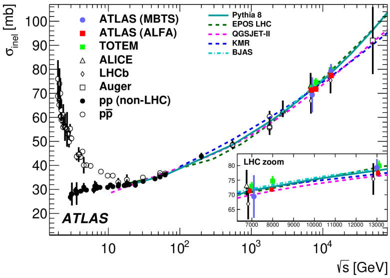

the total inelastic cross section is obtained by subtraction of the total elastic cross section from the total cross section

comparison of inelastic cross-section measurements with other published measurements and model predictions as a function of the centre-of-mass energy

total inelastic cross section in agreement with previous ATLAS measurements using MBTS detectors

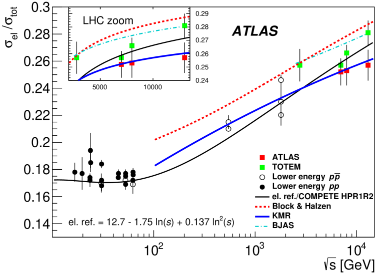

σ_{el}/σ_{tot} at different centre-of-mass energies compared to model predictions and to a conventional parameterization of the elastic cross section divided by the COMPETE of σ_{tot}

Energy evolution of σ_{tot} and ρ

Energy evolution of the total cross section and of the ρ-parameter compared to different model predictions

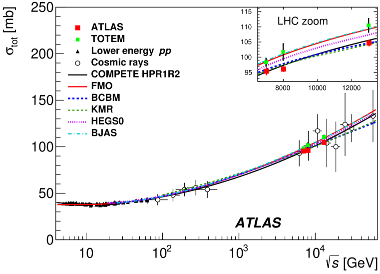

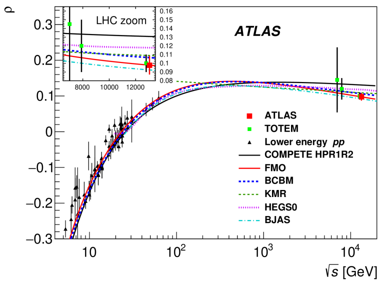

ALFA and TOTEM difference in $\sigma_{tot} \approx 2.2$ σ (similar trend seen at 7 and 8 TeV)

result incompatible with COMPETE (community-standard semi-empirical fits, predicted $\rho \simeq 0.13$) indicating Odderon exchange or a slowdown of σ_{tot} rise at high $\sqrt{s}$

Energy evolution of B

- nuclear slope parameter B related to the slope of the Pomeron Regge trajectory α'
- the increase of the B slope corresponds to a reduction of the emission cone of elastically scattered particles: "shrinkage of the forward cone"

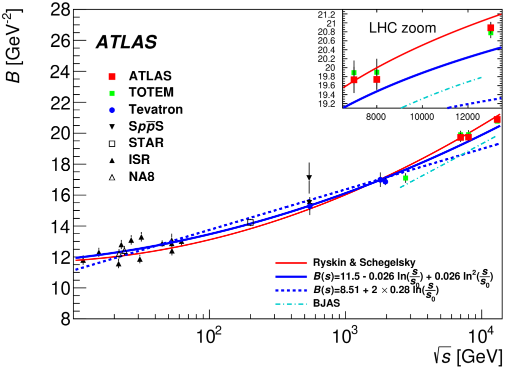

a quadratic energy evolution appears to be favoured by the data

but: the selection of lower-energy data has a significant impact on the shape of the evolution $\Rightarrow$ the fit including all data does not give a perfect description of the LHC data

Conclusions

Elastic results

$$\sigma_{tot}(pp \to X) = 104.68 \pm 1.080.0085\ (exp.) \pm 0.12\ (th.)\ mb$$
$$\rho = 0.0978 \pm 0.0085\ (exp.) \pm 0.0064\ (th.)$$
$$B = 21.14 \pm 0.13\ GeV^{-2}$$
$$C = -6.7 \pm 2.2\ GeV^{-4}$$
$$D = 17.4 \pm 7.8\ GeV^{-6}$$

- most precise measurement of σ_{tot} at 13 TeV
- the low value of ρ and the measurement of σ_{tot} are in tension with standard evolution models like COMPETE
- measurements of σ_{tot} at ATLAS are systematically lower than the results from TOTEM (5.9 mb, 2.2 σ at 13 TeV). The difference is mostly in the normalization
- more details about this analysis on ArXiv

Backup

t-reconstruction

Subtraction method

in elastic scattering the particles are back-to-back $\Rightarrow$ the scattering angles on the A-side and C-side are the same in magnitude and opposite in sign, the protons originate from the same vertex

$$\theta_w^\star = \frac{w_A - w_C}{M_{12,A} + M_{12,C}}$$

Local angle method

local angle θ_w of the tracks measured between the inner and outer stations on the same side

$$\theta_w^\star = \frac{\theta_{w,A} - \theta_{w,C}}{M_{22,A} + M_{22,C}}$$

t-reconstruction

Local subtraction method

using measurements at the inner (237 m) and the outer (245 m) stations, separately on the A-side and C-side, then combining the two sides

$$\theta^{\star}_{w,S} = \frac{M^{245}_{11,S} \times w_{237,S} - M^{237}_{11,S} \times w_{245,S}}{M^{245}_{11,S} \times M^{237}_{12,S} - M^{237}_{11,S} \times M^{245}_{12,S}}, \quad S = A, C$$

Lattice method

using both the measured positions and the local angle to reconstruct the scattering angle by the inversion of the transport matrix

$$\begin{pmatrix} w^{\star} \\ \theta^{\star}_{w} \end{pmatrix} = M^{-1} \begin{pmatrix} w \\ \theta_{w} \end{pmatrix}$$